

Exploiting lymphatic transport and complement activation in nanoparticle vaccines

Sai T Reddy¹, André J van der Vlies¹, Eleonora Simeoni¹, Veronique Angeli^{2,4}, Gwendalyn J Randolph², Conlin P O'Neil¹, Leslie K Lee¹, Melody A Swartz^{1,3} & Jeffrey A Hubbell^{1,3}

Antigen targeting^{1–5} and adjuvancy schemes^{6,7} that respectively facilitate delivery of antigen to dendritic cells and elicit their activation have been explored in vaccine development. Here we investigate whether nanoparticles can be used as a vaccine platform by targeting lymph node–residing dendritic cells via interstitial flow and activating these cells by *in situ* complement activation. After intradermal injection, interstitial flow transported ultra-small nanoparticles (25 nm) highly efficiently into lymphatic capillaries and their draining lymph nodes, targeting half of the lymph node–residing dendritic cells, whereas 100-nm nanoparticles were only 10% as efficient. The surface chemistry of these nanoparticles activated the complement cascade, generating a danger signal *in situ* and potentially activating dendritic cells. Using nanoparticles conjugated to the model antigen ovalbumin, we demonstrate generation of humoral and cellular immunity in mice in a size- and complement-dependent manner.

Technologies for presentation of protein or peptide antigens as vaccines must address two fundamental issues: efficient delivery of antigen to dendritic cells and subsequent dendritic cell activation to trigger adaptive immunity. Strategies for antigen delivery have recently focused on *in vivo* targeting of dendritic cells through the use of monoclonal antibodies either fused with protein^{1,2,4} or grafted to the surface of microparticles³. Such strategies often target peripheral dendritic cells in skin. Antigen delivery to lymph nodes might provide an attractive alternative, because dendritic cells are present in much higher concentration in these lymph nodes. To initiate adaptive immunity, adjuvants must induce dendritic cell maturation. Dendritic cells are often matured by ‘danger signals’ that work through pathways of innate immunity such as activation of Toll-like receptors (TLRs) and inflammatory cytokine receptors. Whereas experimental vaccines using danger signals have shown promise^{6,7}, risk of toxicity, physiological transport limitations and economic feasibility remain as potentially limiting issues.

As a nanoparticulate platform for antigen delivery, we used Pluronic-stabilized polypropylene sulfide (PPS) nanoparticles⁸.

These nanoparticles have a hydrophobic core of crosslinked PPS, which degrades by becoming water soluble under oxidative conditions

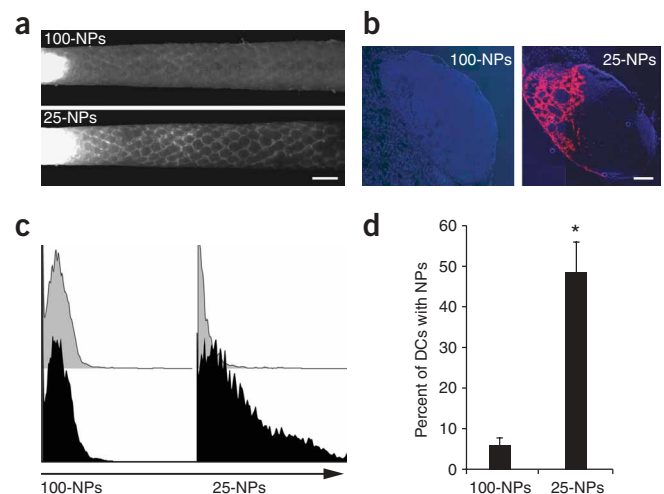


Figure 1 Ultra-small nanoparticles accumulate in lymph nodes after intradermal injection, whereas slightly larger ones do not. **(a)** Fluorescence microlymphangiography is convenient for imaging lymphatic uptake because the lymphatic capillaries all drain in one direction, toward the base of the tail. Shown is a co-infusion into mouse-tail skin with 100- and 25-nm fluorescently labeled nanoparticles (100- and 25-NPs, respectively) where the 25-NPs enter the dermal lymphatic capillary network much more efficiently than 100-NPs do. Scale bar, 1 mm. **(b)** The 25-nm, but not the 100-nm, nanoparticles are visible in mouse lymph node sections 24 h after injection. Cell nuclei shown in blue (DAPI); scale bar, 200 μ m. Images in **a** and **b** are representative of at least three independent experiments. **(c)** Flow cytometry histograms show CD11c⁺ dendritic cells isolated from the draining lymph nodes after intradermal co-injection of fluorescently labeled 100- and 25-NPs (black) or phosphate-buffered saline (PBS) control (gray). Results are representative of at least three independent experiments. **(d)** Calculations of the fraction of dendritic cells that have internalized NPs after a co-injection as in **c** supports the hypothesis that lymph node dendritic cells are effectively targeted after intradermal injection of smaller but not larger nanoparticles. Values are the means from six independent experiments; error bars correspond to s.d. *, $P < 0.001$.

¹Institute of Bioengineering, École Polytechnique Fédérale de Lausanne (EPFL), CH-1015 Lausanne, Switzerland. ²Department of Gene and Cell Medicine, Mount Sinai School of Medicine, New York, New York, 10029 USA. ³Institute of Chemical Sciences and Engineering, École Polytechnique Fédérale de Lausanne (EPFL), CH-1015 Lausanne, Switzerland. ⁴Present address: Department of Microbiology, Immunology Programme, National University of Singapore, Singapore 117456. Correspondence and request for materials should be addressed to M.A.S (melody.swartz@epfl.ch) or J.A.H (jeffrey.hubbell@epfl.ch).

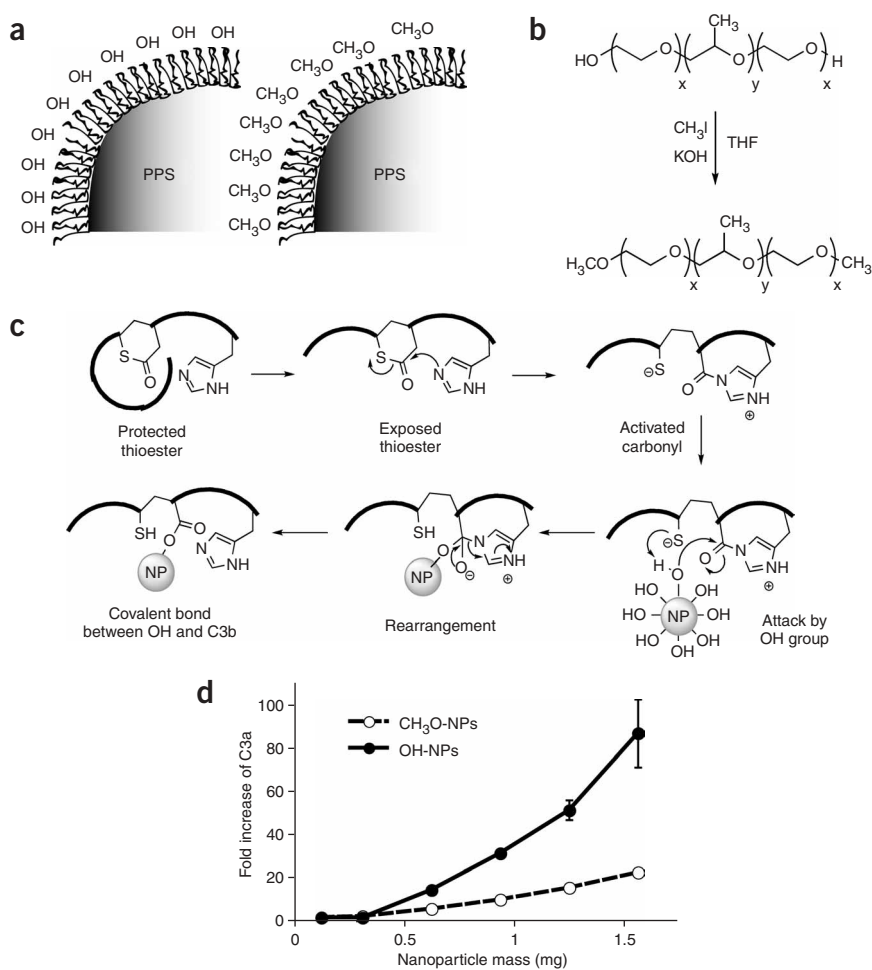


Figure 2 Polyhydroxylated nanoparticle surfaces activate complement. **(a)** Synthesis and stabilization with two different forms of Pluronic allowed the generation of polyhydroxylated- or polymethoxylated-nanoparticles. **(b)** The α,ω -terminal OH groups on Pluronic could be converted to OCH₃ groups. **(c)** The proposed mechanism where OH groups on the polyhydroxylated nanoparticles can bind to the exposed thioester of C3b to activate complement by the alternative pathway. **(d)** Nanoparticle-induced complement activation, as measured through C3a presence in human serum after incubation with nanoparticles, was demonstrated to be high with polyhydroxylated nanoparticles but low with polymethoxylated nanoparticles (OH- and CH₃O-NPs, respectively). Results are normalized to control of serum incubation with PBS. Values are means of three independent experiments; error bars correspond to standard error of mean, s.e.m.

(such as those found within the lysosome), and a hydrophilic surface corona of Pluronic, a block copolymer of polyethylene glycol and polypropylene glycol⁸. The Pluronic enables good size control down to ~20 nm during inverse emulsion polymerization⁸. By selecting the lymph node as our target, we seek to achieve localization of the nanoparticles where dendritic cells exist in high concentrations and where a substantial fraction of dendritic cells are phenotypically and functionally immature⁹ and thus able to process new antigen. This is in contrast to the common approach of targeting dendritic cells in peripheral tissues like skin or muscle¹⁰, where dendritic cells reside in much lower numbers and must travel to the lymph node after antigen uptake¹¹, permitting premature antigen presentation¹². To compensate for low dendritic cell density in peripheral tissues, many investigators have explored biomolecular approaches to dendritic cell targeting. Whereas particles can be taken up nonspecifically by peripheral dendritic cells, as demonstrated with polymer microparticles

containing antigen-encoding DNA^{5,13}, virus-like particles¹⁴ or polystyrene nanobeads¹⁵, investigators have also conjugated monoclonal antibodies directed to dendritic cell-surface receptors such as DEC205 or 33D1 to protein antigen^{1,2} or to the surface of liposomes or microparticles^{3,16} for more specific targeting. However, such sophisticated cell-specific targeting may not be necessary if antigen could be delivered to the lymph node, where dendritic cells are present in high numbers.

To target dendritic cells in the lymph node, we exploited a biophysical mechanism—interstitial flow—to access the lymphatic system as a low-resistance delivery route that leads to lymph nodes. The lymphatic system constantly drains fluid and macromolecules from the interstitial space, creating small interstitial flows on the order of 0.1–1 $\mu\text{m/s}$ ^{17,18}. We take advantage of this basic physiological phenomenon by using nanoparticles that are so small that they are convected by this interstitial flow through the interstitial matrix into the draining lymphatic capillary bed. In previous work, size was shown to be the most critical factor affecting lymphatic uptake of particle-based delivery vehicles¹⁹, probably based on the network structure of the interstitial extracellular matrix and the valve-like overlapping lymphatic cell-cell junctions, through which entry of particles depends on extracellular matrix hydration¹⁷. Larger nanoparticles have also been explored by others²⁰, but these enter the lymphatics much less efficiently than ultra-small nanoparticles and therefore are likely to target peripheral more than lymph node-resident dendritic cells.

To explore lymphatic uptake, we performed fluorescence microlymphangiography²¹ by constant pressure infusion of nanoparticles into the tip of mouse tail skin; 25-nm but not 100-nm nanoparticles were quickly and efficiently taken up by

lymphatic vessels (**Fig. 1a**). Once within the lymphatic vasculature, the 25-nm nanoparticles were efficiently transported to the draining lymph node (**Fig. 1b**) and could be retained there for at least 120 h after injection, were colocalized exclusively with macrophages and dendritic cells in the subcapsular sinus, and were not found within T- or B-cell zones¹⁹. The 25-nm nanoparticles were found within ~50% of dendritic cells isolated from the lymph node (**Fig. 1c,d**), whereas 100-nm nanoparticles were found within only 6% of dendritic cells and could not be visualized within the draining lymph node after 24 h (**Fig. 1b–d**). It is likely that these larger nanoparticles entered the lymph node after internalization by peripheral dendritic cells and migration to the node, because dendritic cells take up large particles in this size range as efficiently as smaller particles^{5,19}. Thus, in addition to targeting peripheral dendritic cells in skin, nanoparticles that are small enough to readily access the lymphatic system from the interstitium can effectively target lymph node-resident dendritic cells.

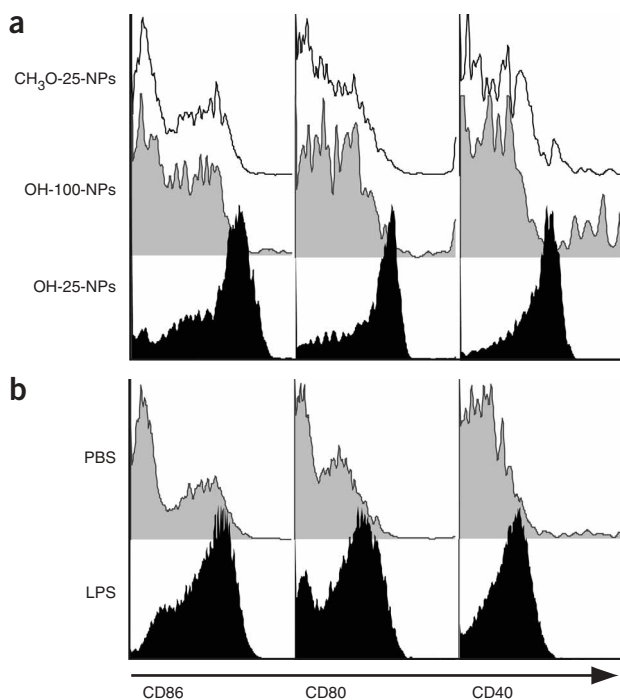


Figure 3 Lymph node-targeting, complement-activating nanoparticles induce dendritic cell maturation *in vivo*. **(a)** Flow cytometry histograms showing CD11c⁺ dendritic cells isolated from mouse lymph nodes at 24 h after intradermal injection with either 25-nm polymethoxylated nanoparticles (CH₃O-25-NPs), 100-nm polyhydroxylated-NPs (OH-100-NPs), or 25-nm polyhydroxylated-NPs (OH-25-NPs) demonstrate selective activation: OH-25-NPs, which both target lymph nodes and strongly activate complement, induce upregulation of the dendritic cell maturation markers CD86, CD80 and CD40. **(b)** Histograms are also shown from mice that received injections of negative and positive controls, PBS and LPS, respectively; demonstrating that activation with OH-25-NPs is comparable to activation with LPS. All results are representative of at least three independent experiments.

Next, we designed the nanoparticles to function themselves as an adjuvant, which is necessary to induce dendritic cell maturation and initiate adaptive immunity. Adjuvants are typically danger signals that work by activation of TLRs and inflammatory cytokine receptors; such adjuvants have been widely explored in experimental vaccine formulations^{6,7}. For example, molecular danger signals that mimic the effect of the endotoxin lipopolysaccharide (LPS), such as monophosphoryl lipid A, have been explored⁷, as well as the cytokines CD40 ligand and interferon (IFN)- γ ^{1,2,16}. Delivery of danger signals with antigen by co-encapsulation in liposomes^{3,16}, packaging into virus-like particles¹⁴ or co-injection with dendritic cell-targeting antibody fusion proteins^{1,4,22} have been successful at producing adaptive immune responses, but despite such promising results, many complexities remain including toxicity, physiological transport and economic feasibility. As an alternative adjuvant strategy, we explored the possibility of using the complement cascade as a danger signal of innate immunity, designing our nanoparticles with a surface chemistry that spontaneously induces complement activation *in situ*.

Because the use of adjuvants based on known TLR activators has dominated vaccine research in recent years⁷, the complement system, another pathway of innate immunity, has been relatively unexplored as a danger signal adjuvant. Complement primarily serves as a biochemical defense system that clears pathogens nonspecifically, but it can also play a role in promoting antigen-specific immune responses²³. Its ability to enhance humoral immunity has been exploited with molecular targeting adjuvants that enhance antigen delivery directly to B cells²⁴. Only recently has it been discovered that complement can promote T-cell immunity^{25,26}, but the molecular mechanisms and interactions with dendritic cells remain largely unidentified.

In the alternative pathway of the complement cascade, C3 is activated by spontaneous proteolytic cleavage to form the C3a and C3b fragments. C3b undergoes a conformational change and exposes a thioester, which forms a reactive acyl-imidazole bond with a proximate histidine residue. The formed thiolate acts as a base and

catalyzes the transfer of the acyl group to hydroxyl groups, prototypically located on carbohydrate residues that coat pathogens²⁷. This mechanism also occurs with some nonnatural hydroxylated material surfaces^{28,29}, including Pluronic-coated materials³⁰. Biomaterials scientists have typically sought to avoid complement activation in order to minimize effects such as implant rejection and clearance of systemic drug delivery vehicles. Here, we instead attempted to do the opposite and specifically designed a biomaterial that strongly activates complement so that it could generate a molecular adjuvant danger signal *in situ*. Indeed, we saw that nanoparticles stabilized by Pluronic (Fig. 2a) activated complement through Pluronic's α and ω terminal hydroxyl groups (Fig. 2b–d). To explore whether complement was activated exclusively by surface hydroxyls, we synthesized nanoparticles with α,ω -methoxy-Pluronic (Fig. 2b). These activated complement to a much reduced, but still nonzero extent (Fig. 2d), demonstrating that although the surface hydroxyls are critical for very high levels of complement activation, they are not the only feature on the nanoparticle surface involved in complement activation.

With the ability to target lymph node-resident dendritic cells with ultra-small nanoparticles and activate complement with their polyhydroxylated surfaces, we then determined that these properties could be combined to elicit dendritic cell maturation. Following intradermal injection into mouse dorsal foot skin of 25-nm polyhydroxylated-nanoparticles, dendritic cells isolated 24 h after injection from the draining lymph nodes displayed a shift from the immature to the mature phenotype through upregulation of the co-stimulatory molecules CD86, CD80 and CD40 (Fig. 3a). Both lymph node-targeting and complement activation were necessary to elicit such an effect, because 100-nm polyhydroxylated and 25-nm polymethoxylated nanoparticles did not induce dendritic cell maturation above control levels (Fig. 3a). Moreover, the dendritic cell maturation level induced by 25-nm polyhydroxylated nanoparticles was very similar to that induced by the endotoxin LPS, a potent activator of TLR4 (Fig. 3b), further demonstrating that complement activation can be a very effective intrinsic danger signal for dendritic cells. Complement activation did not appear to significantly affect lymph node dendritic cell uptake as 25-nm polymethoxylated and polyhydroxylated nanoparticles were internalized by dendritic cells at similar levels (Supplementary Fig. 1 online). As a comparison we also injected commercially available 20-nm polystyrene nanospheres (Invitrogen) with carboxylated surfaces. The polystyrene nanospheres accumulated in lymph nodes at similar levels as 25-nm polyhydroxylated nanoparticles but did not induce dendritic cell maturation (Supplementary Fig. 2 online). Thus, nanoparticles engineered to both target lymph nodes and strongly activate complement are potent maturation stimuli for dendritic cells.

To test the extent to which the lymph node-targeting, complement-activating nanoparticles induced an antigen-specific immune

response, we conjugated ovalbumin, a model protein antigen, to nanoparticle surfaces (**Supplementary Fig. 3** online). Ovalbumin conjugation did not significantly affect the nanoparticle size and the antigen remained coupled to the particle after delivery to the lymph node (**Supplementary Fig. 4** online). Furthermore, the 25-nm ovalbumin nanoparticles induced lymph node dendritic cell maturation at the same levels as unconjugated ovalbumin co-injected with LPS (**Fig. 4a**). To measure T-cell proliferation, we used an adoptive transfer experiment with OT-II mice (a transgenic mouse strain in which CD4

T cells upregulate their ovalbumin-specific T-cell receptors). Consistent with the results on dendritic cell activation, the 25-nm polyhydroxylated-ovalbumin-nanoparticles showed nearly the same capacity to induce T-cell proliferation as the positive control of ovalbumin co-injected with LPS, each producing approximately seven daughter generations (**Fig. 4b**). Helper CD4 T cells play an important role in initiating cellular immunity by differentiating cytotoxic CD8 T cells and in humoral immunity by stimulating B cells to produce antibodies. Therefore nanoparticle induction of strong antigen-specific CD4 T-cell proliferation provided the impetus to determine if cellular and humoral immunity could be induced.

Cellular immunity is critical for vaccines capable of inducing resistance to intracellular pathogens, and this is typically defined by the induction of cytotoxic T-cell memory. This is often measured by determining if CD8 T cells from immunized mice become activated, producing the inflammatory cytokine IFN- γ after reexposure to an antigenic stimulus. Adjuvants that produce sufficient CD8 T-cell activation have thus far been elusive, however, an LPS synthetic derivative, monophosphoryl lipid A has shown potential⁷. Thus, we measured the ability of ultra-small, ovalbumin-conjugated, polyhydroxylated nanoparticles to induce cellular immunity compared to LPS. We found that 25-nm polyhydroxylated-ovalbumin-nanoparticles produced activated T cells at similar levels to unconjugated ovalbumin co-injected with LPS, and at significantly higher levels than 25-nm polymethoxylated-ovalbumin-nanoparticles (**Fig. 4c**). This demonstrated that downstream antigen-specific cellular immunity was attained with ovalbumin nanoparticles, but only when the complement-activating surface was present.

Another critical feature of vaccines is the ability to induce humoral immunity, the generation of a resistant level of circulating antibodies against a pathogenic antigen. To determine whether the nanoparticles could induce humoral immunity, we measured antibody titers in serum 21 d after a single injection. We found that 25-nm polyhydroxylated-ovalbumin-nanoparticles produced strong levels of anti-ovalbumin IgG similar to injections of ovalbumin with LPS or the clinically used adjuvant alum. Significantly lower antibody titers were observed with 100-nm polyhydroxylated-ovalbumin-nanoparticles and 25-nm polymethoxylated-ovalbumin-nanoparticles (**Fig. 4d**). As further confirmation of the importance of complement activation, we found that C3^{-/-} mice produced substantially lower antibody titers when injected with 25-nm polyhydroxylated-ovalbumin-nanoparticles than did wild-type controls (**Fig. 4d**), where injections of ovalbumin

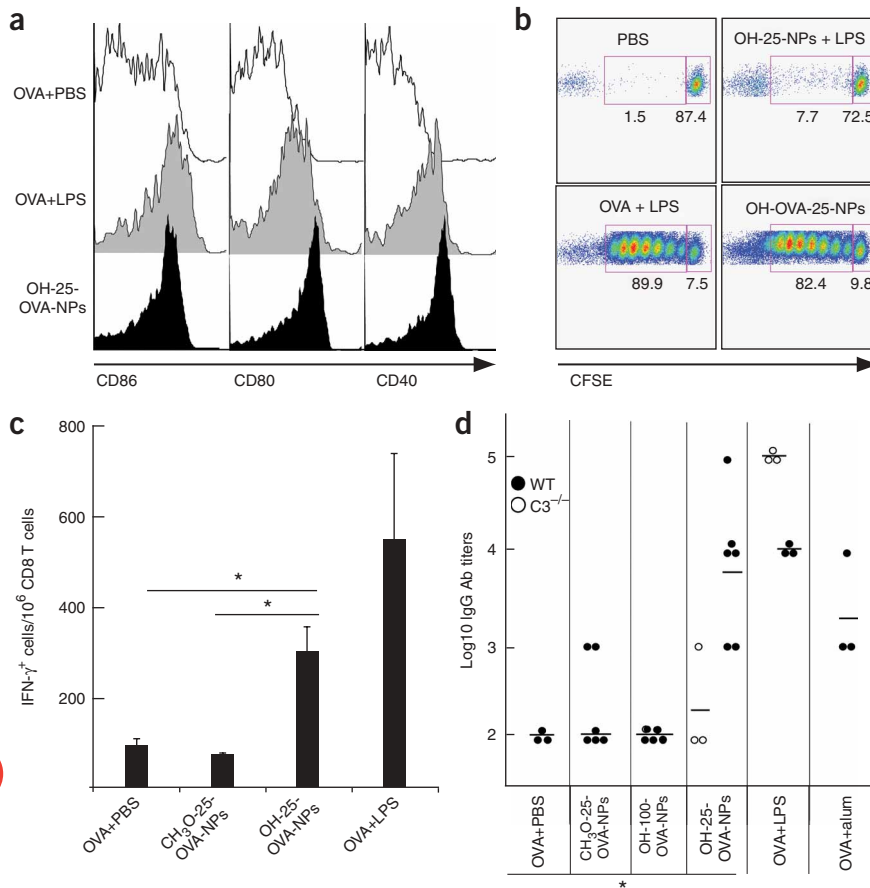


Figure 4 Lymph node-targeting, complement-activating nanoparticles induce antigen-specific adaptive immune responses. **(a)** Histograms display lymph node CD11c⁺ dendritic cell maturation profiles after intradermal injections into mice with either ovalbumin with PBS or LPS (+PBS or +LPS, respectively) or ovalbumin conjugated to 25-nm polyhydroxylated nanoparticles (OH-25-ovalbumin-NPs). Dendritic cell activation is apparent for the OH-25-ovalbumin nanoparticles, comparable to that obtained with ovalbumin+LPS. **(b)** Flow cytometry profiles show that lymph node CD4⁺CD45.2⁺ T-cell proliferation after treatment with OH-25-ovalbumin-NPs is comparable to that after treatment with ovalbumin+LPS as measured by dilution of 5-(6)-carboxyfluorescein diacetate succinimidyl diester (CFSE) labeled OT-II T cells. Results from **a** and **b** are representative of two to four independent experiments. **(c)** A restimulation assay was used to determine CD8 T-cell memory by IFN- γ production. Mice received various intradermal injections of antigen and nanoparticle formulations. The graph shows CD8 T-cell memory after treatment with OH-25-ovalbumin-NPs but not CH₃O-25-ovalbumin-NPs. Results are mean values from three mice in each group; error bars correspond to s.e.m. *, $P < 0.05$. **(d)** Mice received single injections of different antigen and nanoparticle formulations, and serum was collected 21 d after injection. The graph shows antibody titers for anti-ovalbumin IgG, where each point represents an individual mouse and the bar represents the group mean. A strong humoral immune response was observed only for OH-25-ovalbumin-NPs, but not larger or low-complement activating nanoparticles. When the OH-25-ovalbumin-NPs were injected into C3^{-/-} mice (open circles, wild type, WT), this response was abrogated (filled circles, wild type, WT), confirming the role of *in situ* complement activation as a danger signal. *, $P < 0.05$.

with LPS resulted in a normal antibody response in C3^{-/-} mice. Thus, ovalbumin nanoparticles could only induce humoral immunity in the presence of both lymph node-targeting and complement activation.

Current vaccine technology research is dominated by strategies targeting peripheral dendritic cells, for example, in the skin or muscle, using molecular principles for dendritic cell targeting. Lymph node-resident dendritic cells are rarely considered as targets. Thus far, research with particulate systems in a size range small enough for lymphatic uptake such as virus-like particles¹⁴ and polystyrene nanobeads¹⁵ has not exploited lymphatic transport. Lymphatic delivery is often even prevented by aggregating antigen with alum to produce a depot effect. Adjuvant research is dominated by formulations using TLR activators and inflammatory cytokines as molecular danger signals^{6,7}, complement activation having been relatively unexplored. Our results highlight two alternative strategies for vaccination: interstitial-to-lymphatic flow to deliver antigen and adjuvant to lymph node-resident dendritic cells, and *in situ* complement activation to mature these cells. Whereas we present the nanoparticle system here as an implementation to explore these concepts, we do note its ease of fabrication and antigen conjugation, high stability and attractive affordability. Nevertheless, questions regarding toxicity, elimination and molecular interaction between complement and dendritic cells remain to be addressed to demonstrate the reported system as more than an implementation to explore these two strategies.

METHODS

Animals. BALB/c, C57BL6 and C3^{-/-} (B6.129S4-C3tm1Crr/J), OT-II Tg (CD45.2) and CD45.1 mice (Jackson Immunoresearch) at 6–10 weeks old and weighing 20–30 g, were used for this study. All protocols were approved by the Veterinary Authorities of the Canton Vaud according to Swiss law (protocol number nos. 1687 and 1954) and by the Institutional Animal Use and Care Committee of Mt. Sinai School of Medicine.

Nanoparticle synthesis. Pluronic-stabilized PPS nanoparticles with diameters of 25 and 100 nm were synthesized by inverse emulsion polymerization as described elsewhere⁸.

Antigen-conjugated nanoparticles. Antigen conjugation to PPS nanoparticles was accomplished by functionalizing Pluronic F-127 surface with the model protein antigen, ovalbumin. The conjugation scheme began with synthesis of Pluronic divinylsulfone, to which ovalbumin was coupled through a free thiol group on ovalbumin in a Michael-type addition reaction. Pluronic vinylsulfone conjugated to ovalbumin was then blended with conventional Pluronic and nanoparticles were synthesized as usual.

Fluorescence microlymphangiography. A constant-pressure infusion of fluorescently labeled nanoparticles was performed as previously described¹⁹ in order to visualize the lymphatic capillary network in the tail skin of mice.

C3a detection. A C3a sandwich enzyme-linked immunosorbent assay (ELISA) was performed to measure complement activation in human serum after incubation with polyhydroxylated- or polymethoxylated nanoparticles.

CD4 T-cell proliferation. T cells from OT-II mice were isolated and labeled with 5-(6)-carboxyfluorescein diacetate succinimidyl diester (CFSE) and were then adoptively transferred into wild-type (WT) mice. After 2 d, control, antigen or nanoparticle treatments were injected into mice. At 5 d, lymph node cells were isolated and the dilution of CFSE was measured by flow cytometry.

CD8 T-cell memory. Mice received various intradermal injections of antigen and nanoparticle formulations into dorsal foot skin, with a booster at 7 d and

at 21 d. T cells were isolated from the draining lymph node, exposed to an ovalbumin-specific major histocompatibility-I peptide, and IFN- γ production was measured through ELISPOT.

Ovalbumin antibody titers. A direct ELISA against ovalbumin was performed to detect the presence of anti-ovalbumin IgG in mouse serum.

Additional methods. Detailed methods are available in the **Supplementary Methods** online.

Note: Supplementary information is available on the Nature Biotechnology website.

ACKNOWLEDGMENTS

We thank M. Pasquier, V. Borel, V. Garea for valuable technical assistance; J.M. Rutkowski for scientific discussions; J.B. Dixon for MATLAB programming. Project funded by the Competence Centre for Materials Science and Technology (CCMX) of the ETH-Board, Switzerland (to M.A.S. and J.A.H.).

AUTHOR CONTRIBUTIONS

S.T.R. designed and performed the research, analyzed the data and wrote the manuscript; A.J.v.d.V. synthesized materials and analyzed synthetic data; E.S. developed methods on T-cell activation and analyzed the data; V.A. performed the research on T-cell adoptive transfer, analyzed the data and provided useful discussion on interpretation; G.J.R. analyzed the data and provided useful discussion on interpretation; C.P.O. synthesized materials and analyzed synthetic data; L.K.L. developed methods on T-cell activation and antibody titer measurement; M.A.S. designed the research, analyzed the data and wrote the manuscript; J.A.H. designed the research, analyzed the data and wrote the manuscript.

COMPETING INTERESTS STATEMENT

The authors declare competing financial interests: details accompany the full-text HTML version of the paper at <http://www.nature.com/naturebiotechnology/>.

Published online at <http://www.nature.com/naturebiotechnology/>

Reprints and permissions information is available online at <http://npg.nature.com/reprintsandpermissions>

- Bonifaz, L.C. *et al.* *In vivo* targeting of antigens to maturing dendritic cells via the DEC-205 receptor improves T cell vaccination. *J. Exp. Med.* **199**, 815–824 (2004).
- Dudziak, D. *et al.* Differential antigen processing by dendritic cell subsets in vivo. *Science* **315**, 107–111 (2007).
- Kwon, Y.J., James, E., Shastri, N. & Frechet, J.M. *In vivo* targeting of dendritic cells for activation of cellular immunity using vaccine carriers based on pH-responsive microparticles. *Proc. Natl. Acad. Sci. USA* **102**, 18264–18268 (2005).
- Trumpfheller, C. *et al.* Intensified and protective CD4+ T cell immunity in mice with anti-dendritic cell HIV gag fusion antibody vaccine. *J. Exp. Med.* **203**, 607–617 (2006).
- Wang, C. *et al.* Molecularly engineered poly(ortho ester) microspheres for enhanced delivery of DNA vaccines. *Nat. Mater.* **3**, 190–196 (2004).
- O'Hagan, D.T. & Valiante, N.M. Recent advances in the discovery and delivery of vaccine adjuvants. *Nat. Rev. Drug Discov.* **2**, 727–735 (2003).
- Ulevitch, R.J. Therapeutics targeting the innate immune system. *Nat. Rev. Immunol.* **4**, 512–520 (2004).
- Rehor, A., Hubbell, J.A. & Tirelli, N. Oxidation-sensitive polymeric nanoparticles. *Langmuir* **21**, 411–417 (2005).
- Wilson, N.S. *et al.* Most lymphoid organ dendritic cell types are phenotypically and functionally immature. *Blood* **102**, 2187–2194 (2003).
- Reddy, S.T., Swartz, M.A. & Hubbell, J.A. Targeting dendritic cells with biomaterials: developing the next generation of vaccines. *Trends Immunol.* **27**, 573–579 (2006).
- Randolph, G.J., Angeli, V. & Swartz, M.A. Dendritic-cell trafficking to lymph nodes through lymphatic vessels. *Nat. Rev. Immunol.* **5**, 617–628 (2005).
- Pack, D.W. Timing is everything. *Nat. Mater.* **3**, 133–134 (2004).
- Little, S.R. *et al.* Poly-beta amino ester-containing microparticles enhance the activity of nonviral genetic vaccines. *Proc. Natl. Acad. Sci. USA* **101**, 9534–9539 (2004).
- Storni, T. *et al.* Nonmethylated CG motifs packaged into virus-like particles induce protective cytotoxic T cell responses in the absence of systemic side effects. *J. Immunol.* **172**, 1777–1785 (2004).
- Fifis, T. *et al.* Size-dependent immunogenicity: therapeutic and protective properties of nano-vaccines against tumors. *J. Immunol.* **173**, 3148–3154 (2004).
- van Broekhoven, C.L., Parish, C.R., Demangel, C., Britton, W.J. & Altin, J.G. Targeting dendritic cells with antigen-containing liposomes: a highly effective procedure for induction of antitumor immunity and for tumor immunotherapy. *Cancer Res.* **64**, 4357–4365 (2004).

17. Swartz, M.A. The physiology of the lymphatic system. *Adv. Drug Deliv. Rev.* **50**, 3–20 (2001).
18. Swartz, M.A. & Fleury, M.E. Interstitial flow and its effects in soft tissues. *Annu. Rev. Biomed. Eng.* **9**, 229–256 (2007).
19. Reddy, S.T., Rehor, A., Schmoekel, H.G., Hubbell, J.A. & Swartz, M.A. In vivo targeting of dendritic cells in lymph nodes with poly(propylene sulfide) nanoparticles. *J. Control. Release* **112**, 26–34 (2006).
20. Nishioka, Y. & Yoshino, H. Lymphatic targeting with nanoparticulate system. *Adv. Drug Deliv. Rev.* **47**, 55–64 (2001).
21. Reddy, S.T., Berk, D.A., Jain, R.K. & Swartz, M.A. A sensitive in vivo model for quantifying interstitial convective transport of injected macromolecules and nanoparticles. *J. Appl. Physiol.* **101**, 1162–1169 (2006).
22. Boscardin, S.B. *et al.* Antigen targeting to dendritic cells elicits long-lived T cell help for antibody responses. *J. Exp. Med.* **203**, 599–606 (2006).
23. Carroll, M.C. The complement system in regulation of adaptive immunity. *Nat. Immunol.* **5**, 981–986 (2004).
24. Dempsey, P.W., Allison, M.E., Akkaraju, S., Goodnow, C.C. & Fearon, D.T. C3d of complement as a molecular adjuvant: bridging innate and acquired immunity. *Science* **271**, 348–350 (1996).
25. Kemper, C. & Atkinson, J.P. T-cell regulation: with complements from innate immunity. *Nat. Rev. Immunol.* **7**, 9–18 (2007).
26. Kopf, M., Abel, B., Gallimore, A., Carroll, M. & Bachmann, M.F. Complement component C3 promotes T-cell priming and lung migration to control acute influenza virus infection. *Nat. Med.* **8**, 373–378 (2002).
27. Gadjeva, M. *et al.* The covalent binding reaction of complement component C3. *J. Immunol.* **161**, 985–990 (1998).
28. Tang, L., Liu, L. & Elwing, H.B. Complement activation and inflammation triggered by model biomaterial surfaces. *J. Biomed. Mater. Res.* **41**, 333–340 (1998).
29. Nilsson, B., Ekdahl, K.N., Mollnes, T.E. & Lambris, J.D. The role of complement in biomaterial-induced inflammation. *Mol. Immunol.* **44**, 82–94 (2007).
30. Kidane, A. & Park, K. Complement activation by PEO-grafted glass surfaces. *J. Biomed. Mater. Res.* **48**, 640–647 (1999).